Available online at www.sciencedirect.com

ScienceDirect

IFAC PapersOnLine 50-1 (2017) 7923–7928

Collision-Free Formation Control for Multiple Quadrotor-Manipulator Systems ⋆

Yuhua Qi, Jianan Wang and Jiayuan Shan

School of Aerospace Engineering, Beijing Institute of Technology, Beijing, China (e-mail: wangjianan@ieee.org).

Abstract: In this paper, we develop a formation control law with collision avoidance for multiple quadrotor-manipulator systems that each quadrotor is equipped with a robotic manipulator. Firstly, the kinematic and dynamic models of a quadrotor with multi-DOF robotic manipulator are built together using Euler-Lagrange (EL) equations. Based on the aggregated dynamic model, we propose a control scheme consisting of position controller, attitude controller and manipulator controller, respectively. The desired formation is achieved by the proposed position controller and attitude controller, while the collision avoidance is guaranteed by an artificial potential function (APF) method. The robotic manipulators are able to perform cooperative missions by the proposed manipulator controller. The overall stability of the closed-loop system is proven by a Lyapunov method and Matrosov's theorem. In the end, the proposed control scheme is demonstrated by a formation flying mission of four quadrotors with 2-DOF manipulators.

Keywords: Formation Control, Collision Avoidance, Quadrotor, Robotic Manipulator

1. INTRODUCTION

Unmanned Aerial Vehicles (UAVs) have been widely witnessed in both military and civilian applications, such as aerial surveillance, agricultural irrigation and aerial photography, etc. Due to the superior mobility of UAVs, much interest is attracted to utilize them for mobile manipulation such as aerial transportation in remote areas or reparation of hard-to-reach structures. To this end, robotic manipulator can be equipped on the UAVs to enhance the manipulation function where ground robotic vehicles are inaccessible.

When equipping the robotic manipulator on the quadrotor platform, the dynamics of the robotic manipulator are highly coupled with the quadrotor, which should be carefully considered in the controller design for the overall system. Many research groups have begun studying quadrotor-manipulator system, such as Lippiello and Ruggiero (2012), Arleo et al. (2013), Yang and Lee (2014), Khalifa et al. (2013) and Naldi et al. (2015). Moreover, it would be even better if multiple quadrotor-manipulator systems that each quadrotor equipped with a robotic manipulator execute a complicated task cooperatively. Compared to the single quadrotor-manipulator system, it can significantly improve the performance of the system and enhance the robustness so that the application field of the overall system would be dramatically expanded. Various research works focus on the cooperative control of the networked EL systems (Ren (2009), Chung and Slotine (2007), Chen et al. (2013), Qi et al. (2016)). Although the dynamic model of the quadrotor-manipulator system is in the EL formalism, the above method cannot be applied into the whole system directly because the quadrotor is underactuated. However, to our best knowledge, there is no research on the cooperative control of multiple quadrotor-manipulator systems. In the scenario of multi-agent systems, collision avoidance is apparently vital for the success of the whole mission. It becomes more severe to avoid collision in the multiple quadrotor-manipulator systems, especially. The APF method is a real-time collision avoidance strategy that computes the avoidance control inputs as obstacles are detected (Stipanovic et al. (2007), Wang and Xin (2013)).

In this paper, we address the general EL dynamic model of the quadrotor equipped with a multi-DOF manipulator. Based on the dynamic model of the integrated system, the control scheme including position controller, attitude controller and manipulator controller are proposed. The proposed position controller is designed to drive multiple quadrotors to form a desired formation and guarantee collision avoidance which is achieved by an APF method. The proposed attitude controller is designed for attitude stabilization of the quadrotor and the proposed manipulator controller is designed via contraction theory to make each manipulator reach the desired joint angles cooperatively.

The rest of this paper is organized as follows. In Section 2, we introduce the kinematic and dynamic models of the integrated system. The control scheme of the multiple quadrotor-manipulator systems is described in Section 3. Section 4 provides simulation results. Finally, Section 5 concludes this paper.

Throughout this paper, we let $\mathbb{R}$ be the set of real numbers. Let $\mathcal{G}$ be a weighted undirected graph of order n with the set of nodes $\mathcal{V} = \{1, ..., n\}$, set of edges $\mathcal{E} \subseteq \mathcal{V} \times \mathcal{V}$,

⋆ This work is supported by NSFC Grant No.61503025 and Research Fund of Key Laboratory within Ministry of Industry and Information.

10.1016/j.ifacol.2017.08.764

and a weighted adjacency matrix $\mathcal{A} = [a_{ij}] \in \mathbb{R}^{n\times n}$ with nonnegative adjacency elements a_{ij}. Weighted adjacency matrix $\mathcal{A}$ is defined such that $a_{ij} = a_{ji}$ is a positive weight if $(i,j) \in \mathcal{E}$, while $a_{ij} = 0$ if $(i,j) \notin \mathcal{E}$. Let Laplacian matrix $\mathcal{L} = [l_{ij}] \in \mathbb{R}^{n\times n}$ associated with $\mathcal{A}$ be defined as $l_{ii} = \sum_{j=1,j\neq i}^{n} a_{ij}$ and $l_{ij} = -a_{ij}$, where $i \neq j$. Accordingly, if $\mathcal{G}$ is connected and undirected, then $(\mathcal{L} \otimes I_p)\boldsymbol{x} = 0$ or $\boldsymbol{x}^T(\mathcal{L} \otimes I_p) = 0$ if and only if $\boldsymbol{x}_i = \boldsymbol{x}_j$, where $\boldsymbol{x}_i \in \mathbb{R}^p$, $\boldsymbol{x} = [\boldsymbol{x}_1; \ldots; \boldsymbol{x}_n]$. Note that $\boldsymbol{x}^T(\mathcal{L} \otimes I_p)\boldsymbol{x} = \frac{1}{2}\sum_{i=1}^{n}\sum_{j=1}^{n} a_{ij}\|\boldsymbol{x}_i - \boldsymbol{x}_j\|^2$.

2. SYSTEM MODELING

In this section, the kinematics and dynamics of the quadrotor-manipulator system are presented in a general version.

2.1 Kinematics

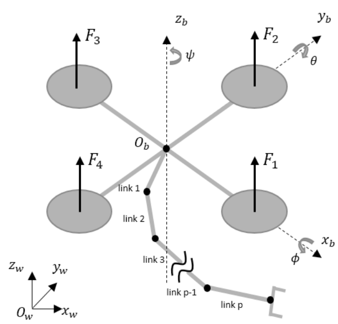

Fig. 1. The quadrotor-manipulator system with corresponding frames

Consider a quadrotor-manipulator system consisting of a quadrotor with a p-DOF manipulator as shown in Fig. 1. Let $\sum_w$ denotes the world-fixed inertial reference frame, $\sum_b$ denotes the quadrotor body-fixed reference frame. $\boldsymbol{p}_q = [x; y; z] \in \mathbb{R}^3$ is the position of the mass center of the quadrotor in $\sum_w$. With the roll/pitch/yaw angles of the quadrotor represented by $\boldsymbol{\phi} = [\varphi; \theta; \psi] \in \mathbb{R}^3$, the rotation matrix R_b from $\sum_b$ to $\sum_w$ is given as

$$R_b = \begin{bmatrix} c_\theta c_\psi - s_\varphi s_\theta s_\psi & -c_\varphi s_\psi & s_\theta c_\psi + s_\varphi c_\theta s_\psi \\ c_\theta s_\psi + s_\varphi s_\theta c_\psi & c_\varphi c_\psi & s_\theta s_\psi - s_\varphi c_\theta c_\psi \\ -c_\varphi s_\theta & s_\varphi & c_\varphi c_\theta \end{bmatrix}, \quad (1)$$

where c_γ and s_γ denote, respectively, $\cos\gamma$ and $\sin\gamma$. Moreover, let $\dot{\boldsymbol{p}}_q$ denotes linear velocity of the quadrotor and $\boldsymbol{\omega} = [\omega_x; \omega_y; \omega_z] \in \mathbb{R}^3$ denotes angular velocity of the quadrotor which can be represented by $\boldsymbol{\omega} = Q\dot{\boldsymbol{\phi}}$. Q is the transformation matrix between the time derivative of $\boldsymbol{\phi}$ and angular velocity.

The generalized variables of the quadrotor-manipulator system can be given as $\boldsymbol{q} = [\boldsymbol{p}_q; \boldsymbol{\phi}; \boldsymbol{\alpha}] \in \mathbb{R}^{6+p}$ where $\boldsymbol{\alpha} = [\alpha_1; \alpha_2; \ldots; \alpha_p] \in \mathbb{R}^p$, α_i is the joint angle of link i of manipulator. We can easily obtain the kinematics of the quadrotor as follows:

$$\dot{\boldsymbol{p}}_q = \mathrm{diag}[I_{3\times 3}, 0_{3\times 3}, 0_{p\times p}]\dot{\boldsymbol{q}},\ \boldsymbol{w} = \mathrm{diag}[0_{3\times 3}, Q, 0_{p\times p}]\dot{\boldsymbol{q}}, \quad (2)$$

where $I_{n\times n}$ is the $n \times n$ identity matrix and $0_{n\times n}$ is the $n \times n$ null matrix. Let $\boldsymbol{p}_{l_i}$ denotes the mass center position of the link i of the manipulator with respect to $\sum_w$ and $\boldsymbol{\omega}_{l_i}$ denotes angular velocity of link i of the manipulator. It is straightforward to obtain

$$\boldsymbol{p}_{l_i} = \boldsymbol{p}_q + R_b\boldsymbol{p}_{l_i}^b,\ \boldsymbol{\omega}_{l_i} = \boldsymbol{\omega} + R_b\boldsymbol{\omega}_{l_i}^b, \quad (3)$$

where $\boldsymbol{p}_{l_i}^b$ is the mass center position of the link i of the manipulator with respect to $\sum_b$ and $\boldsymbol{\omega}_{l_i}^b$ is the relative angular velocity between the link i and the frame $\sum_b$. According to Siciliano et al. (2009), the following relationship holds

$$\dot{\boldsymbol{p}}_{l_i}^b = J_{P_i}\dot{\boldsymbol{\alpha}},\ \boldsymbol{\omega}_{l_i}^b = J_{O_i}\dot{\boldsymbol{\alpha}}, \quad (4)$$

where J_{P_i} and J_{O_i} are the translation and rotation Jacobians, respectively. With the equation (3) and (4), we can obtain the kinematics of the link i of the manipulator

$$\dot{\boldsymbol{p}}_{l_i} = \dot{\boldsymbol{p}}_q - S(R_b\boldsymbol{p}_{l_i}^b)\boldsymbol{\omega} + R_bJ_{P_i}\dot{\boldsymbol{\alpha}}, \quad (5)$$

$$\boldsymbol{\omega}_{l_i} = \boldsymbol{\omega} + R_bJ_{O_i}\dot{\boldsymbol{\alpha}}, \quad (6)$$

where $S(\cdot)$ is the skew-symmetric matrix operator performing the cross product and we apply the fact that $\dot{R}_b = S(\boldsymbol{\omega})R_b$ (Siciliano et al. (2009)). With the equation (2), (5) and (6), the translational and angular velocities of the quadrotor and each link of the manipulator in $\sum_w$ are mapped by $\boldsymbol{q}$ and $\dot{\boldsymbol{q}}$.

2.2 Dynamics

To derive the dynamic model of the integrated system, the EL equations are applied as follows:

$$\frac{d}{dt}\frac{\partial L}{\partial \dot{\boldsymbol{q}}} - \frac{\partial L}{\partial \boldsymbol{q}} = \boldsymbol{u},\ L = K - U, \quad (7)$$

where L is the Lagrangian with kinetic energy K and potential energy U of the integrated system, $\boldsymbol{u}$ is the generalized input.

For the quadrotor-manipulator system considered in the previous subsection, the total kinetic energy K and its components are computed as follows:

$$K = K_q + \sum_{i=1}^{p} K_{l_i}, \quad (8)$$

$$K_q = \tfrac{1}{2}m_q\dot{\boldsymbol{p}}_q^T\dot{\boldsymbol{p}}_q + \tfrac{1}{2}\boldsymbol{\omega}^TR_bI_qR_b^T\boldsymbol{\omega}, \quad (9)$$

$$K_{l_i} = \tfrac{1}{2}m_{l_i}\dot{\boldsymbol{p}}_{l_i}^T\dot{\boldsymbol{p}}_{l_i} + \tfrac{1}{2}\boldsymbol{\omega}_{l_i}^TR_bR_{l_i}^bI_{l_i}R_b^{l_i}R_b^T\boldsymbol{\omega}_{l_i}, \quad (10)$$

where m_q is the mass of quadrotor, m_{l_i} is the mass of link i of manipulator, I_q is the inertia matrix of quadrotor, I_{l_i} is the inertia matrix of link i of manipulator. $R_{l_i}^b$ is the rotation matrix from the frame associated to the mass center of the link i to $\sum_b$ and $R_b^{l_i}=(R_{l_i}^b)^T$. Likewise, the total potential energy of the integrated system is described as follows:

$$U = U_q + \sum_{i=1}^{p} U_{l_i}, \quad (11)$$

$$U_q = m_qg\boldsymbol{e}_3^T\boldsymbol{p}_q,\ U_{l_i} = m_{l_i}g\boldsymbol{e}_3^T(\boldsymbol{p}_q + R_b\boldsymbol{p}_{l_i}^b), \quad (12)$$

where U_q denotes the potential energy of the quadrotor and U_{l_i} denotes the potential energy of the link i of the manipualtor. $\boldsymbol{e}_3$ is the unit vector $[\,0\ 0\ 1\,]^T$ and g is the gravity constant.

By substituting (8)-(12) into (7), the dynamic model of the quadrotor-manipulator system can be derived as the following

$$M(\boldsymbol{q})\ddot{\boldsymbol{q}} + C(\boldsymbol{q},\dot{\boldsymbol{q}})\dot{\boldsymbol{q}} + G(\boldsymbol{q}) = \boldsymbol{u}, \quad (13)$$

where $M(\boldsymbol{q}) \in \mathbb{R}^{(6+p)\times(6+p)}$ is the symmetric positive-definite inertia matrix. $C(\boldsymbol{q},\dot{\boldsymbol{q}}) \in \mathbb{R}^{(6+p)\times(6+p)}$ is the Coriolis matrix. $G(\boldsymbol{q}) \in \mathbb{R}^{(6+p)}$ represents gravity effects.

Note that we have $\dot{M}(\boldsymbol{q}) - 2C(\boldsymbol{q}, \dot{\boldsymbol{q}})$ is skew-symmetric. The total kinetic energy can be expressed by the inertia matrix $M(\boldsymbol{q})$ as

$$K = \tfrac{1}{2}\dot{\boldsymbol{q}}^T M(\boldsymbol{q})\dot{\boldsymbol{q}}. \quad (14)$$

By substituting equations (8)-(12) into (14), the inertia matrix $M(\boldsymbol{q})$ is computed as the following equation,

$$M(\boldsymbol{q}) = \begin{bmatrix} M_{11} & M_{12} & M_{13} \\ M_{21} & M_{22} & M_{23} \\ M_{31} & M_{32} & M_{33} \end{bmatrix}, \quad (15)$$

$$M_{11} = \left(m_q + \sum_{i=1}^{p} m_{l_i}\right) I_{3\times3}, \quad (16)$$

$$M_{22} = Q^T R_b I_q {R_b}^T Q + \sum_{i=1}^{p} \left(m_{l_i} Q^T S(\boldsymbol{p}_{l_i}^b)^T S(\boldsymbol{p}_{l_i}^b) Q + +Q^T R_b R_{l_i}^b I_{l_i} (R_{l_i}^b)^T {R_b}^T Q\right), \quad (17)$$

$$M_{33} = \sum_{i=1}^{p} \left(m_{l_i} {J_{p_i}}^T J_{p_i} + {J_{O_i}}^T R_{l_i}^b I_{l_i} (R_{l_i}^b)^T J_{O_i}\right), \quad (18)$$

$$M_{12} = M_{21}^T = -\sum_{i=1}^{p} \left(m_{l_i} R_b S(\boldsymbol{p}_{l_i}^b) Q\right), \quad (19)$$

$$M_{13} = M_{31}^T = \sum_{i=1}^{p} (m_{l_i} R_b J_{p_i}), \quad (20)$$

$$M_{23} = M_{32}^T = \sum_{i=1}^{p} \left(Q^T R_b R_{l_i}^b I_{l_i} (R_{l_i}^b)^T J_{O_i} - m_{l_i} Q^T S(\boldsymbol{p}_{l_i}^b)^T J_{p_i}\right), \quad (21)$$

where we apply the fact that $RS(\boldsymbol{\omega}) R^T = S(R\boldsymbol{\omega})$ if R is a rotation matrix. The Coriolis matrix $C(\boldsymbol{q}, \dot{\boldsymbol{q}})$ can be derived by calculating each element with the following equation (Siciliano et al. (2009))

$$c_{ij} = \sum_{k=1}^{6+p} \tfrac{1}{2} \left(\tfrac{\partial m_{ij}}{\partial q_k} + \tfrac{\partial m_{ik}}{\partial q_j} - \tfrac{\partial m_{jk}}{\partial q_i}\right) \dot{q}_k, \quad (22)$$

where m_{ij} is the element of the inertia matrix $M(\boldsymbol{q})$. $G(\boldsymbol{q})$ is calculated with the following partial derivative

$$G(\boldsymbol{q}) = \tfrac{\partial U}{\partial \boldsymbol{q}}. \quad (23)$$

We rewrite (13) in the vector form as

$$\begin{bmatrix} M_{11} & M_{12} & M_{13} \\ M_{21} & M_{22} & M_{23} \\ M_{31} & M_{32} & M_{33} \end{bmatrix} \begin{bmatrix} \ddot{\boldsymbol{p}}_q \\ \ddot{\boldsymbol{\phi}} \\ \ddot{\boldsymbol{\alpha}} \end{bmatrix} + \begin{bmatrix} C_{11} & C_{12} & C_{13} \\ C_{21} & C_{22} & C_{23} \\ C_{31} & C_{32} & C_{33} \end{bmatrix} \begin{bmatrix} \dot{\boldsymbol{p}}_q \\ \dot{\boldsymbol{\phi}} \\ \dot{\boldsymbol{\alpha}} \end{bmatrix} + \begin{bmatrix} G_1 \\ G_2 \\ G_3 \end{bmatrix} = \begin{bmatrix} \boldsymbol{u}_f \\ \boldsymbol{u}_\tau \\ \boldsymbol{u}_\alpha \end{bmatrix}, \quad (24)$$

where $\boldsymbol{u}_f$, $\boldsymbol{u}_\tau$, $\boldsymbol{u}_\alpha$ are the generalized inputs corresponding to $\boldsymbol{p}_q$, $\boldsymbol{\phi}$, $\boldsymbol{\alpha}$ respectively. $\boldsymbol{u}_\alpha = \left[u_{\alpha_1}, \ldots, u_{\alpha_p}\right]^T \in \mathbb{R}^p$ is the input vector of the manipulator actuation troques which can be actuated directly through joint actuators. Since the quadrotor is an underactuated system, $\boldsymbol{u}_f$ and $\boldsymbol{u}_\tau$ need to be transformed to the quadrotor input, $\boldsymbol{F} = [F_1; F_2; F_3; F_4] \in \mathbb{R}^4$, the thrusts of the four motors of the quadrotor as follows:

$$\begin{bmatrix} \boldsymbol{u}_f \\ \boldsymbol{u}_\tau \\ \boldsymbol{u}_\alpha \end{bmatrix} = \begin{bmatrix} R_b & 0 & 0 \\ 0 & Q^T & 0 \\ 0 & 0 & I_{p\times p} \end{bmatrix} \begin{bmatrix} \Omega & 0 \\ 0 & I_{p\times p} \end{bmatrix} \begin{bmatrix} \boldsymbol{F} \\ \boldsymbol{u}_\alpha \end{bmatrix}, \quad (25)$$

$$\Omega = \begin{bmatrix} 0 & 0 & 0 & 0 \\ 0 & 0 & 0 & 0 \\ 1 & 1 & 1 & 1 \\ 0 & d & 0 & -d \\ -d & 0 & d & 0 \\ c & -c & c & -c \end{bmatrix}, \quad (26)$$

where d is the distance from a motor to the mass center of the quadrotor and c is the drag factor.

3. CONTROL SCHEME

This section depicts the control method design of the multiple quadrotor-manipulator systems. Consider n quadrotor-manipulator systems, (13) is represented by

$$M_i(\boldsymbol{q}_i)\ddot{\boldsymbol{q}}_i + C(\boldsymbol{q}_i, \dot{\boldsymbol{q}}_i)\dot{\boldsymbol{q}}_i + G_i(\boldsymbol{q}_i) = \boldsymbol{u}_i, \; i \in N = \{1, \ldots, n\}. \quad (27)$$

For each individual system, the dynamics can be divided into position loop, attitude loop and manipulator loop as follows:

$$M_{11,i}\ddot{\boldsymbol{p}}_i + M_{12,i}\ddot{\boldsymbol{\phi}}_i + M_{13,i}\ddot{\boldsymbol{\alpha}}_i + C_{11,i}\dot{\boldsymbol{p}}_i + C_{12,i}\dot{\boldsymbol{\phi}}_i + C_{13,i}\dot{\boldsymbol{\alpha}}_i + G_{1,i} = \boldsymbol{u}_{f,i}, \quad (28)$$

$$M_{21,i}\ddot{\boldsymbol{p}}_i + M_{22,i}\ddot{\boldsymbol{\phi}}_i + M_{23,i}\ddot{\boldsymbol{\alpha}}_i + C_{21,i}\dot{\boldsymbol{p}}_i + C_{22,i}\dot{\boldsymbol{\phi}}_i + C_{23,i}\dot{\boldsymbol{\alpha}}_i + G_{2,i} = \boldsymbol{u}_{\tau,i}, \quad (29)$$

$$M_{31,i}\ddot{\boldsymbol{p}}_i + M_{32,i}\ddot{\boldsymbol{\phi}}_i + M_{33,i}\ddot{\boldsymbol{\alpha}}_i + C_{31,i}\dot{\boldsymbol{p}}_i + C_{32,i}\dot{\boldsymbol{\phi}}_i + C_{33,i}\dot{\boldsymbol{\alpha}}_i + G_{3,i} = \boldsymbol{u}_{\alpha,i}. \quad (30)$$

where $\boldsymbol{p}_i$ denotes the position of the mass center of the ith quadrotor.

Define the overall avoidance region and the avoidance regions for each pair of quadrotors as

$$\Gamma = \textstyle\bigcup_{i,j} \Gamma_{ij}, \; \Gamma_{ij} = \{\boldsymbol{p} : \boldsymbol{p} \in \mathbb{R}^3, \|\boldsymbol{p}_i - \boldsymbol{p}_j\| \le r\}. \quad (31)$$

Also define the overall detection region and the detection regions for each pair of quadrotors

$$\Psi = \textstyle\bigcup_{i,j} \Psi_{ij}, \; \Psi_{ij} = \{\boldsymbol{p} : \boldsymbol{p} \in \mathbb{R}^3, \|\boldsymbol{p}_i - \boldsymbol{p}_j\| \le R\}, \quad (32)$$

where $R > r > 0$, R denotes the radius of the region in which agents can detect the presence of other quadrotors, r denotes the smallest safe distance between the quadrotors.

We assume that each quadrotor-manipulator system is equipped with a sensing device and a communication device. The sensing device can detect other quadrotors if other quadrotors enter the detection region. On the other hand, the communication device is used to communicate between the quadrotors. The task of the multiple quadrotor-manipulator systems is divided in three steps, 1) multiple quadrotors form a desired formation cooperatively without collision from any arbitrary initial position, 2) each quadrotor can hover in the air stably and 3) each manipulator can reach a desired joint angle cooperatively to finalize a specified task.

We present the main result of this paper and the proof follows in three steps.

Theorem 1. Consider the multiple quadrotor-manipulator systems (28)-(30) with a ring-structured communication topology, the collision-free formation can be achieved via (36), (55) and (62): 1) $\boldsymbol{p}_i - \boldsymbol{p}_j \to \boldsymbol{\delta}_i - \boldsymbol{\delta}_j$, $\dot{\boldsymbol{p}}_i \to \boldsymbol{0}$, $\forall i \neq j \in N$, 2) $\boldsymbol{\phi}_i \to \boldsymbol{0}$, $\dot{\boldsymbol{\phi}}_i \to \boldsymbol{0}$, $\forall i \in N$ and 3) $\boldsymbol{\alpha}_i \to \boldsymbol{\alpha}_{d,i}$, $\dot{\boldsymbol{\alpha}}_i \to \boldsymbol{0}$, $\forall i \in N$, if $K_{\boldsymbol{p},i} > 0$, $K_{\boldsymbol{\phi},i} > 0$, $K^1_{\boldsymbol{\alpha},i} > 0$, $K^2_{\boldsymbol{\alpha},i} > 0$ and $K^1_{\boldsymbol{\alpha},i} - 2K^2_{\boldsymbol{\alpha},i} > 0$. $\boldsymbol{\delta}_i$ denotes the formation offset vector of the ith quadrotor and $\boldsymbol{\alpha}_{d,i}$ is the desired joint angle of ith manipulator.

3.1 Position Control

In the position loop, our goal is to guarantee multiple quadrotors forming a formation without collisions. To this end, let us define the following avoidance function (Stipanovic et al. (2007))

$$\mathrm{V}_{ij}(\boldsymbol{p}_i,\boldsymbol{p}_j) = (\min\left\{0, \frac{\|\boldsymbol{p}_i - \boldsymbol{p}_j\|^2 - R^2}{\|\boldsymbol{p}_i - \boldsymbol{p}_j\|^2 - r^2}\right\})^2, \; \forall i \neq j \in N. \quad (33)$$

The partial derivative of V_{ij} with respect to $\boldsymbol{p}_i$ is given by

$$\frac{\partial V_{ij}}{\partial \boldsymbol{p}_i} = \begin{cases} 0 & \|\boldsymbol{p}_i - \boldsymbol{p}_j\| \ge R, \\ 4\dfrac{(R^2 - r^2)(\|\boldsymbol{p}_i - \boldsymbol{p}_j\|^2 - R^2)}{(\|\boldsymbol{p}_i - \boldsymbol{p}_j\|^2 - r^2)^3}(\boldsymbol{p}_i - \boldsymbol{p}_j) & R > \|\boldsymbol{p}_i - \boldsymbol{p}_j\| > r, \\ \text{not defined} & \|\boldsymbol{p}_i - \boldsymbol{p}_j\| = r, \\ 0 & \|\boldsymbol{p}_i - \boldsymbol{p}_j\| < r. \end{cases} \quad (34)$$

Since the functions $\mathrm{V}_{ij}(\boldsymbol{p}_i,\boldsymbol{p}_j)$ are symmetric with respect to their arguments, it is easy to obtain

$$\frac{\partial V_{ij}}{\partial \boldsymbol{p}_i} = -\frac{\partial V_{ij}}{\partial \boldsymbol{p}_j} = \frac{\partial V_{ji}}{\partial \boldsymbol{p}_i} = -\frac{\partial V_{ji}}{\partial \boldsymbol{p}_j}. \quad (35)$$

Our goal is to guarantee that the trajectory of each quadrotor avoids the region Γ. To this end, the following position control law is proposed for the ith quadrotor-manipulator system

$$\begin{aligned}\boldsymbol{u}_{f,i} =& M_{12,i}\ddot{\boldsymbol{\phi}}_i+M_{13,i}\ddot{\boldsymbol{\alpha}}_i+C_{12,i}\dot{\boldsymbol{\phi}}_i+C_{13}\dot{\boldsymbol{\alpha}}_i+G_{1,i}-\sum_{j=1}^{n}\frac{\partial V_{ij}}{\partial \boldsymbol{p}_i}\\ &-\sum_{j=1}^{n}a_{ij}[(\boldsymbol{p}_i-\boldsymbol{p}_j)-(\boldsymbol{\delta}_i-\boldsymbol{\delta}_j)]-\sum_{j=1}^{n}b_{ij}\left(\dot{\boldsymbol{p}}_i-\dot{\boldsymbol{p}}_j\right)-K_{\boldsymbol{p},i}\dot{\boldsymbol{p}}_i,\end{aligned} \tag{36}$$

where a_{ij} is the (i,j) entry of weighted adjacency matrix $\mathcal{A}\in\mathbb{R}^{n\times n}$ associated with graph $\mathcal{G}_A$ for q_i, b_{ij} is the (i,j) entry of weighted adjacency matrix $\mathcal{B}\in\mathbb{R}^{n\times n}$ associated with graph $\mathcal{G}_B$ for $\dot{\boldsymbol{q}}_i$ and $K_{\boldsymbol{p},i}\in\mathbb{R}^{3\times 3}$ is a symmetric matrix. Note that here $\mathcal{G}_A$ and $\mathcal{G}_B$ are allowed to be different.

Theorem 2. Given the position loop of the multiple quadrotor-manipulator systems (28), the formation can be achieved with collision avoidance under the controller in (34) and (36), i.e., $\boldsymbol{p}_i-\boldsymbol{p}_j\to\boldsymbol{\delta}_i-\boldsymbol{\delta}_j$, $\dot{\boldsymbol{p}}_i\to\boldsymbol{0}$, $\forall i\neq j\in N$ as $t\to\infty$, if graph $\mathcal{G}_A$ and graph $\mathcal{G}_B$ are undirected and connected and $K_{\boldsymbol{p},i}>0$.

Proof. Let $\boldsymbol{w}_i=\boldsymbol{p}_i-\boldsymbol{\delta}_i$, $\dot{\boldsymbol{w}}_i=\dot{\boldsymbol{p}}_i-\dot{\boldsymbol{\delta}}_i=\dot{\boldsymbol{p}}_i$, $\boldsymbol{w}=\left[\boldsymbol{w}_1^T,\ldots,\boldsymbol{w}_n^T\right]^T$, $\dot{\boldsymbol{w}}=\left[\dot{\boldsymbol{w}}_1^T,\ldots,\dot{\boldsymbol{w}}_n^T\right]^T$, $\bar{M}_{11}=\operatorname{diag}\left[M_{11,1},\ldots,M_{11,n}\right]$, $\bar{C}_{11}=\operatorname{diag}\left[C_{11,1},\ldots,C_{11,n}\right]$, $K_{\boldsymbol{p}}=\operatorname{diag}\left[K_{\boldsymbol{p},1},\ldots,K_{\boldsymbol{p},n}\right]$, $\nabla=\left[\sum_{j=1}^{n}\frac{\partial V_{1j}}{\partial \boldsymbol{p}_1};\ldots;\sum_{j=1}^{n}\frac{\partial V_{nj}}{\partial \boldsymbol{p}_n}\right]$. Using (36), (28) can be written in vector form as

$$\bar{M}_{11}\ddot{\boldsymbol{w}}+\bar{C}_{11}\dot{\boldsymbol{w}}=-(\mathcal{L}_A\otimes I_{3\times3})\boldsymbol{w}-(\mathcal{L}_B\otimes I_{3\times3})\dot{\boldsymbol{w}}-K_{\boldsymbol{p}}\dot{\boldsymbol{w}}-\nabla, \tag{37}$$

where $\mathcal{L}_A$, $\mathcal{L}_B$ are the Laplacian matrix associated with $\mathcal{G}_A$ and $\mathcal{G}_B$ respectively. Using (36), (28) can also written as

$$\tfrac{d}{dt}(\boldsymbol{w}_i-\boldsymbol{w}_j)=\dot{\boldsymbol{w}}_i-\dot{\boldsymbol{w}}_j, \tag{38}$$

$$\begin{aligned}\frac{d}{dt}\dot{\boldsymbol{w}}_i=-M_{11,i}^{-1}\Bigg[&C_{11,i}\dot{\boldsymbol{w}}_i+\sum_{j=1}^{n}a_{ij}(\boldsymbol{w}_i-\boldsymbol{w}_j)\\ &+\sum_{j=1}^{n}b_{ij}\left(\dot{\boldsymbol{w}}_i-\dot{\boldsymbol{w}}_j\right)+K_{\boldsymbol{p},i}\dot{\boldsymbol{w}}_i+\sum_{j=1}^{n}\frac{\partial V_{ij}}{\partial \boldsymbol{p}_i}\Bigg].\end{aligned} \tag{39}$$

Let $\tilde{\boldsymbol{w}}$ be a column stack vector of all $\boldsymbol{w}_i-\boldsymbol{w}_j$, where $i<j$ and $a_{ij}\neq 0$. Consider a Lyapunov function candidate for (38) and (39) as

$$V_1=\tfrac{1}{2}\boldsymbol{w}^T(\mathcal{L}_A\otimes I_{3\times3})\boldsymbol{w}+\tfrac{1}{2}\dot{\boldsymbol{w}}^T\bar{M}_{11}\dot{\boldsymbol{w}}+\sum_{i=1}^{n}\sum_{j>i}V_{ij}. \tag{40}$$

Because $\boldsymbol{w}^T(\mathcal{L}_A\otimes I_{3\times3})\boldsymbol{w}=\frac{1}{2}\sum_{i=1}^{n}\sum_{j=1}^{n}a_{ij}\|\boldsymbol{w}_i-\boldsymbol{w}_j\|^2$, V_1 is positive definite and decrescent with respect to $\tilde{\boldsymbol{w}}$ and $\dot{\boldsymbol{w}}$. Note that system (38) and (39) are non-autonomous due to the dependence of $C_{11,i}$ on $\boldsymbol{q}_i$. As a result, LaSalle's invariance principle is no longer applicable for (38) and (39). Instead, we apply Matrosov's theorem to prove the theorem(Paden and Panja (1988)). Note that Condition (1) in Matrosov's theorem is satisfied.

The derivative of V_1 with respect to t is given by

$$\begin{aligned}\dot{V}_1=&\dot{\boldsymbol{w}}^T(\mathcal{L}_A\otimes I_{3\times3})\boldsymbol{w}+\dot{\boldsymbol{w}}^T\bar{M}_{11}\ddot{\boldsymbol{w}}+\frac{1}{2}\dot{\boldsymbol{w}}^T\dot{\bar{M}}_{11}\dot{\boldsymbol{w}}\\ &+\sum_{i=1}^{n}\sum_{j>i}\big((\frac{\partial V_{ij}}{\partial \boldsymbol{p}_i})^T\dot{\boldsymbol{p}}_i+(\frac{\partial V_{ij}}{\partial \boldsymbol{p}_j})^T\dot{\boldsymbol{p}}_j\big).\end{aligned} \tag{41}$$

Applying (37), yields,

$$\begin{aligned}\dot{V}_1=&\dot{\boldsymbol{w}}^T(\mathcal{L}_A\otimes I_{3\times3})\boldsymbol{w}+\dot{\boldsymbol{w}}^T\left[-\bar{C}_{11}\dot{\boldsymbol{w}}-(\mathcal{L}_A\otimes I_{3\times3})\boldsymbol{w}\right.\\ &\left.-(\mathcal{L}_B\otimes I_{3\times3})\dot{\boldsymbol{w}}-K_{\boldsymbol{p}}\dot{\boldsymbol{w}}-\nabla\right]+\frac{1}{2}\dot{\boldsymbol{w}}^T\dot{\bar{M}}_{11}\dot{\boldsymbol{w}}\\ &+\sum_{i=1}^{n}\sum_{j>i}\big((\frac{\partial V_{ij}}{\partial \boldsymbol{p}_i})^T\dot{\boldsymbol{p}}_i+(\frac{\partial V_{ij}}{\partial \boldsymbol{p}_j})^T\dot{\boldsymbol{p}}_j\big).\end{aligned} \tag{42}$$

Note that $\dot{\bar{M}}_{11}-2\bar{C}_{11}$ is skew symmetric.

$$\begin{aligned}\dot{V}_1=&-\dot{\boldsymbol{w}}^T(\mathcal{L}_B\otimes I_{3\times3})\dot{\boldsymbol{w}}-\dot{\boldsymbol{w}}^TK_{\boldsymbol{p}}\dot{\boldsymbol{w}}-\dot{\boldsymbol{w}}^T\nabla\\ &+\sum_{i=1}^{n}\sum_{j>i}\big((\frac{\partial V_{ij}}{\partial \boldsymbol{p}_i})^T\dot{\boldsymbol{p}}_i+(\frac{\partial V_{ij}}{\partial \boldsymbol{p}_j})^T\dot{\boldsymbol{p}}_j\big),\end{aligned} \tag{43}$$

$$\begin{aligned}\dot{V}_1=&-\dot{\boldsymbol{w}}^T(\mathcal{L}_B\otimes I_{3\times3})\dot{\boldsymbol{w}}-\dot{\boldsymbol{w}}^TK_{\boldsymbol{p}}\dot{\boldsymbol{w}}-\sum_{i=1}^{n}\sum_{j=1}^{n}\dot{\boldsymbol{p}}_i^T\frac{\partial V_{ij}}{\partial \boldsymbol{p}_i}\\ &+\sum_{i=1}^{n}\sum_{j>i}\big((\frac{\partial V_{ij}}{\partial \boldsymbol{p}_i})^T\dot{\boldsymbol{p}}_i+(\frac{\partial V_{ij}}{\partial \boldsymbol{p}_j})^T\dot{\boldsymbol{p}}_j\big).\end{aligned} \tag{44}$$

As equation (35),

$$-\sum_{i=1}^{n}\sum_{j=1}^{n}\dot{\boldsymbol{p}}_i^T\tfrac{\partial V_{ij}}{\partial \boldsymbol{p}_i}+\sum_{i=1}^{n}\sum_{j>i}\big((\tfrac{\partial V_{ij}}{\partial \boldsymbol{p}_i})^T\dot{\boldsymbol{p}}_i+(\tfrac{\partial V_{ij}}{\partial \boldsymbol{p}_j})^T\dot{\boldsymbol{p}}_j\big)=0. \tag{45}$$

Then,

$$\dot{V}_1=-\dot{\boldsymbol{w}}^T(\mathcal{L}_B\otimes I_{3\times3})\dot{\boldsymbol{w}}-\dot{\boldsymbol{w}}^TK_{\boldsymbol{p}}\dot{\boldsymbol{w}}\leq 0, \tag{46}$$

where we apply the fact that $-\dot{\boldsymbol{w}}^T(\mathcal{L}_B\otimes I_{3\times3})\dot{\boldsymbol{w}}\leq 0$ because graph $\mathcal{G}_B$ is undirected and $K_{\boldsymbol{p}}>0$ because $K_{\boldsymbol{p},i}>0$. Therefore, Condition (2) in Matrosov's theorem is satisfied. Note that (46) implies that $V_1(t)\leq V_1(0),\forall t\geq 0$ and (33) implies that $\lim_{\|\boldsymbol{p}_i-\boldsymbol{p}_j\|\to r^+}V_{ij}\left(\boldsymbol{p}_i,\boldsymbol{p}_j\right)=\infty\quad\forall i,j$, we conclude that the trajectory of the quadrotors will never enter Γ and hence collisions are avoided.

Let $W=\dot{\boldsymbol{w}}^T\bar{M}_{11}(\mathcal{L}_A\otimes I_{3\times3})\boldsymbol{w}$. Then we have

$$|W|<\|\dot{\boldsymbol{w}}\|\left\|\bar{M}_{11}\right\|\|(\mathcal{L}_A\otimes I_{3\times3})\boldsymbol{w}\|. \tag{47}$$

According to (16), $\left\|\bar{M}_{11}\right\|$ is bounded. Because $V_1(t)\leq V_1(0),\forall t\geq 0$, $\tilde{\boldsymbol{w}}$ and $\|\dot{\boldsymbol{w}}\|$ are bounded. Noting that $(\mathcal{L}_A\otimes I_{3\times3})\boldsymbol{w}$ is a column stack vector of all $\sum_{j=1}^{n}a_{ij}\left(\boldsymbol{w}_i-\boldsymbol{w}_j\right)$, $i=1,\ldots,n$, it follows that $\|(\mathcal{L}_A\otimes I_{3\times3})\boldsymbol{w}\|$ is also bounded. Then it thus follows that $|W|$ is bounded along the solution trajectory, implying the Condition (3) in Matrosov's theorem is satisfied. The derivative of W along the solution trajectory of (38) and (39) is

$$\dot{W}=\ddot{\boldsymbol{w}}^T\bar{M}_{11}(\mathcal{L}_A\otimes I_{3\times3})\boldsymbol{w}+\dot{\boldsymbol{w}}^T\dot{\bar{M}}_{11}(\mathcal{L}_A\otimes I_{3\times3})\boldsymbol{w}+\dot{\boldsymbol{w}}^T\bar{M}_{11}(\mathcal{L}_A\otimes I_{3\times3})\dot{\boldsymbol{w}}, \tag{48}$$

$$\begin{aligned}\dot{W}=&-\dot{\boldsymbol{w}}^T\bar{C}_{11}^T(\mathcal{L}_A\otimes I_{3\times3})\boldsymbol{w}-\boldsymbol{w}^T(\mathcal{L}_A^2\otimes I_{3\times3})\boldsymbol{w}-\dot{\boldsymbol{w}}^T(\mathcal{L}_B\mathcal{L}_A\otimes I_{3\times3})\boldsymbol{w}\\ &-\dot{\boldsymbol{w}}^TK_{\boldsymbol{p}}(\mathcal{L}_A\otimes I_{3\times3})\boldsymbol{w}-\nabla^T(\mathcal{L}_A\otimes I_{3\times3})\boldsymbol{w}\\ &+\dot{\boldsymbol{w}}^T\dot{\bar{M}}_{11}(\mathcal{L}_A\otimes I_{3\times3})\boldsymbol{w}+\dot{\boldsymbol{w}}^T\bar{M}_{11}(\mathcal{L}_A\otimes I_{3\times3})\dot{\boldsymbol{w}},\end{aligned} \tag{49}$$

where we apply the property of the Kronecker products in Graham (1981). Note that $\dot{V}_1=0$ implies $\dot{\boldsymbol{w}}=0$. On the set $\left\{(\tilde{\boldsymbol{w}},\dot{\boldsymbol{w}})\,\middle|\,\dot{V}_1=0\right\}$, we have

$$\dot{W}=-\boldsymbol{w}^T(\mathcal{L}_A^2\otimes I_{3\times3})\boldsymbol{w}\leq 0. \tag{50}$$

Note that $\left|\dot{W}\right|=\left\|(\mathcal{L}_A^2\otimes I_{3\times3})\boldsymbol{w}\right\|^2$ is positive definite with respect to $\tilde{\boldsymbol{w}}$. Therefore there exists a class $\mathcal{K}$ function, α, such that $\left|\dot{W}\right|>\alpha\left(\|\tilde{\boldsymbol{w}}\|\right)$ (Khalil (2005)). Also note that $\left|\dot{W}\right|$ does not explicitly depend on t. It follows from Lemma 2.3 in Ren (2009) that Condition (4) in Matrosov's theorem is satisfied. In conclusion, the equilibrium of system (38) and (39) is uniformly asymptotically stable, which implies that $\boldsymbol{p}_i-\boldsymbol{p}_j\to\boldsymbol{\delta}_i-\boldsymbol{\delta}_j$, $\dot{\boldsymbol{p}}_i\to\boldsymbol{0}$ as $t\to\infty$ and the region Γ is avoidable. $\square$

3.2 Attitude Control

Next, $\boldsymbol{u}_\tau$ is designed to achieve the desired attitude of the quadrotor. According to (25), $\boldsymbol{u}_f$ depends on the attitude of the quadrotor via the realtion

$$\begin{bmatrix} u_{f,x} \\ u_{f,y} \\ u_{f,z} \end{bmatrix} = \begin{bmatrix} (\cos\psi sin\theta cos\varphi + sin\psi sin\varphi) f_z \\ (\sin\psi sin\theta cos\varphi - \cos\psi sin\varphi) f_z \\ cos\theta cos\varphi f_z \end{bmatrix}, \tag{51}$$

where $f_z = \|\boldsymbol{u}_f\|$ is the total thrust of the quadrotor respect to $\sum_b$. Therefore, the reference state for the roll and pitch angles can be computed as

$$\varphi_d = \arctan(\tfrac{u_{f,x}\cos\psi + u_{f,y}\sin\psi}{u_{f,z}}), \tag{52}$$

$$\theta_d = \arcsin(\tfrac{u_{f,x}\sin\psi - u_{f,y}\cos\psi}{\|\boldsymbol{u}_f\|}). \tag{53}$$

Remark 1. According to (52) and (53), φ_d and θ_d are calculated by the input of position loop. When the quadrotors arrive at the desired position, or $u_{f,x} = u_{f,y} = 0$, then $\varphi_d = \theta_d = 0$. In the other hand, we always choose $\psi_d = 0$.

Define the auxiliary variables as follows:

$$\boldsymbol{s}_{\boldsymbol{\phi},i} = \dot{\boldsymbol{\phi}}_i - \dot{\boldsymbol{\phi}}_{r,i},\ \dot{\boldsymbol{\phi}}_{r,i} = -\Lambda_{\boldsymbol{\phi}}(\boldsymbol{\phi}_i - \boldsymbol{\phi}_{d,i}), \tag{54}$$

where $\Lambda_{\boldsymbol{\phi}} \in \mathbb{R}^{3\times3}$ is a positive matrix and $\boldsymbol{\phi}_{d,i} = [\varphi_{d,i}; \theta_{d,i}; \psi_{d,i}]$.

Then the attitude control law is proposed for the ith quadrotor-manipulator system as follows:

$$\begin{aligned} \boldsymbol{u}_{\tau,i} =& M_{21,i}\ddot{\boldsymbol{p}}_i + M_{23,i}\ddot{\boldsymbol{\alpha}}_i + C_{21,i}\dot{\boldsymbol{p}}_i + C_{23}\dot{\boldsymbol{\alpha}}_i \\ &+ G_{2,i} + M_{22,i}\ddot{\boldsymbol{\phi}}_{r,i} + C_{22,i}\dot{\boldsymbol{\phi}}_{r,i} - K_{\boldsymbol{\phi},i}\boldsymbol{s}_{\boldsymbol{\phi},i}, \end{aligned} \tag{55}$$

where $K_{\boldsymbol{\phi},i} \in \mathbb{R}^{3\times3}$ is a diagonal matrix.

Theorem 3. Consider the system (29) with (55), the desired attitude can be achieved, i.e., $\boldsymbol{\phi}_i \to \boldsymbol{\phi}_{d,i}$, $\dot{\boldsymbol{\phi}}_i \to \boldsymbol{0}$, $\forall i \in N$ as $t \to \infty$, if $K_{\boldsymbol{\phi},i} > 0$.

Proof. Using (55), (29) can be rewritten as

$$M_{22,i}\dot{\boldsymbol{s}}_{\boldsymbol{\phi},i} + C_{22,i}\boldsymbol{s}_{\boldsymbol{\phi},i} + K_{\boldsymbol{\phi}}\boldsymbol{s}_{\boldsymbol{\phi},i} = 0. \tag{56}$$

Choose a Lyapunov function candidate for (29) as

$$V_2 = \tfrac{1}{2}\boldsymbol{s}_{\boldsymbol{\phi},i}{}^T M_{22,i}\boldsymbol{s}_{\boldsymbol{\phi},i}. \tag{57}$$

Then, the derivative of V is given by

$$\dot{V}_2 = \boldsymbol{s}_{\boldsymbol{\phi},i}{}^T M_{22,i}\dot{\boldsymbol{s}}_{\boldsymbol{\phi},i} + \tfrac{1}{2}\boldsymbol{s}_{\boldsymbol{\phi},i}{}^T \dot{M}_{22,i}\boldsymbol{s}_{\boldsymbol{\phi},i}. \tag{58}$$

By applying (56),

$$\dot{V}_2 = \boldsymbol{s}_{\boldsymbol{\phi},i}{}^T(-C_{22,i}\boldsymbol{s}_{\boldsymbol{\phi},i} - K_{\boldsymbol{\phi},i}\boldsymbol{s}_{\boldsymbol{\phi},i}) + \tfrac{1}{2}\boldsymbol{s}_{\boldsymbol{\phi}}{}^T\dot{M}_{22}\boldsymbol{s}_{\boldsymbol{\phi}}, \tag{59}$$

$$\dot{V}_2 = -\boldsymbol{s}_{\boldsymbol{\phi},i}{}^T K_{\boldsymbol{\phi},i}\boldsymbol{s}_{\boldsymbol{\phi},i} < 0, \tag{60}$$

where we apply the fact that $\dot{M}_{22,i} - 2C_{22,i}$ is skew symmetric. It implies that $\boldsymbol{s}_{\boldsymbol{\phi},i} \to 0$ as $t \to \infty$, which means $\boldsymbol{\phi}_i \to \boldsymbol{\phi}_{d,i}$, $\dot{\boldsymbol{\phi}}_i \to \boldsymbol{0}$ as $t \to \infty$. □

3.3 Manipulator Control

Finally, $\boldsymbol{u}_\alpha$ is designed to cooperatively track the desired joint angles for the manipulators. Define the auxiliary variables as follows:

$$\boldsymbol{s}_{\boldsymbol{\alpha},i} = \dot{\boldsymbol{\alpha}}_i - \dot{\boldsymbol{\alpha}}_{r,i},\ \dot{\boldsymbol{\alpha}}_{r,i} = -\Lambda_{\boldsymbol{\alpha}}(\boldsymbol{\alpha}_i - \boldsymbol{\alpha}_{d,i}), \tag{61}$$

where $\Lambda_{\boldsymbol{\alpha}} \in \mathbb{R}^{p\times p}$ is a positive matrix and $\boldsymbol{\alpha}_{d,i} = [\alpha_{1d,i}; \ldots; \alpha_{pd,i}]$.

Then the manipulator control law is proposed for the ith quadrotor-manipulator system as follows:

$$\begin{aligned} \boldsymbol{u}_{\alpha,i} =& M_{31,i}\ddot{\boldsymbol{p}}_i + M_{32,i}\ddot{\boldsymbol{\phi}}_i + C_{31,i}\dot{\boldsymbol{p}}_i + C_{32}\dot{\boldsymbol{\phi}}_i + G_{3,i} + M_{33,i}\ddot{\boldsymbol{\alpha}}_{r,i} \\ &+ C_{33,i}\dot{\boldsymbol{\alpha}}_{r,i} - K^1_{\boldsymbol{\alpha},i}\boldsymbol{s}_{\boldsymbol{\alpha},i} + K^2_{\boldsymbol{\alpha},i}\boldsymbol{s}_{\boldsymbol{\alpha},i-1} + K^2_{\boldsymbol{\alpha},i}\boldsymbol{s}_{\boldsymbol{\alpha},i+1}, \end{aligned} \tag{62}$$

where $K^1_{\boldsymbol{\alpha},i} \in \mathbb{R}^{p\times p}$ is a feedback gain for the ith manipulator and $K^2_{\boldsymbol{\alpha},i} \in \mathbb{R}^{p\times p}$ is a coupling gain with the adjacent members ($i-1$ and $i+1$).

Remark 3. From the control law (62), the ith robotic manipulator only can receive information from the adjacent manipulators ($i-1$ and $i+1$). In this paper, a two-way ring structured communication topology is adopted for the whole multiple quadrotor-manipulator systems, which also guarantees that graph $\mathcal{G}_A$ and graph $\mathcal{G}_B$ are undirected and connected.

Theorem 4. Consider the system (30) with (62) in a ring-structured communication topology, $\boldsymbol{\alpha}_i \to \boldsymbol{\alpha}_{d,i}$, $\dot{\boldsymbol{\alpha}}_i \to \boldsymbol{0}$, $\forall i \in N$ as $t \to \infty$, if $K^1_{\boldsymbol{\alpha},i} > 0$, $K^2_{\boldsymbol{\alpha},i} > 0$ and $K^1_{\boldsymbol{\alpha},i} - 2K^2_{\boldsymbol{\alpha},i} > 0$.

Proof. The closed-loop system after applying the manipulator controller (62) to (30) can be written as follows:

$$M_{33,i}\dot{\boldsymbol{s}}_{\boldsymbol{\alpha},i} + C_{33,i}\boldsymbol{s}_{\boldsymbol{\alpha},i} + K^1_{\boldsymbol{\alpha},i}\boldsymbol{s}_{\boldsymbol{\alpha},i} - K^2_{\boldsymbol{\alpha},i}\boldsymbol{s}_{\boldsymbol{\alpha},i-1} - K^2_{\boldsymbol{\alpha},i}\boldsymbol{s}_{\boldsymbol{\alpha},i+1} = 0. \tag{63}$$

The following proof is the same as in Qi et al. (2016). □

4. SIMULATION

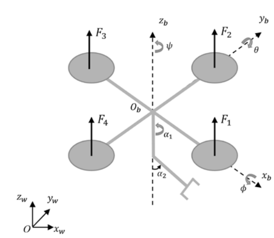

(a) Quadrotor-manipulator system

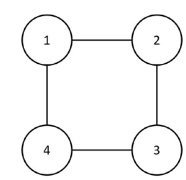

(b) Communication topology

Fig. 2. Quadrotor-manipulator system and communication topology used in simulation

To illustrate the performance of the control scheme, let us consider four quadrotors equipped with a 2-DOF manipulator as shown in Fig. 2(a) hover at $[-15, 0, 5]$ m, $[15, 0.5, 5]$ m, $[0.5, -15, 5]$ m and $[0, 15, 5]$ m. The desired formation is a rhombus and the formation offsets are designed as $\delta_1 = [10, 0, 0]$ m, $\delta_2 = [-10, 0, 0]$ m, $\delta_3 = [0, 10, 0]$ m and $\delta_4 = [0, -10, 0]$ m. In this simulation, we choose $R = 8$ m, $r = 2$ m and desired angles of manipulator are $\alpha_{d,1} = [\pi, \pi/2]^T$ rad, $\alpha_{d,2} = [\pi, \pi/2]^T$ rad, $\alpha_{d,3} = [\pi, \pi/2]^T$ rad and $\alpha_{d,4} = [\pi, \pi/2]^T$ rad. The two-way ring network structure for the four quadrotor-manipulator systems is shown in Fig. 2(b). The physical parameters of the integrated system are given in Table 1.

Table 1. Physical Parameters

Mass of quadrotor m_q	1kg
Length of quadrotor arm l_q	0.4m
Inertia matrix of quadrotor I_q	[1,1,2.48]kg $\times$ m^2
Mass of link j of manipulator $[m_1, m_2]$	[0.3,0.3]kg
Length of link j of manipulator $[l_1, l_2]$	[0.3,0.5]m
Radius of the link 1 r_1	0.03m

The simulation results are presented from Fig. 3 to Fig. 5. For the control gains in the equation (36), (55) and (62), we choose $K_{\boldsymbol{p},i} = \text{diag}\,[5, 5, 5]$, $K_{\boldsymbol{\phi},i} = \text{diag}\,[10, 10, 10]$, $\Lambda_{\boldsymbol{\phi}} = \text{diag}\,[20, 20, 20]$, $K^1_{\boldsymbol{\alpha},i} = \text{diag}\,[5, 5]$, $K^2_{\boldsymbol{\alpha},i} = \text{diag}\,[2, 2]$

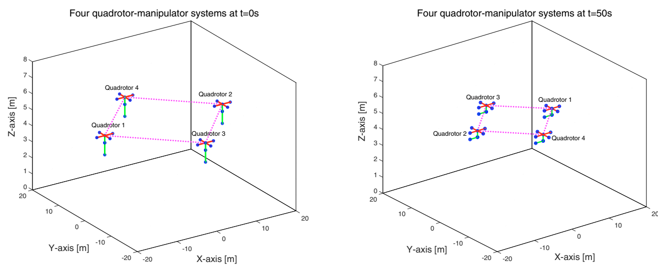

(a) t=0s (b) t=50s

Fig. 3. Four quadrotor-manipulator systems at different time instants

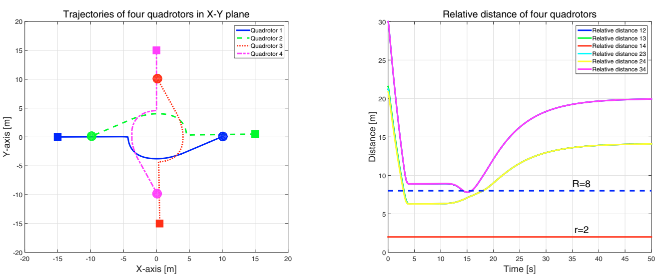

(a) Planar trajectory (b) Relative distance

Fig. 4. Performance of collision avoidance

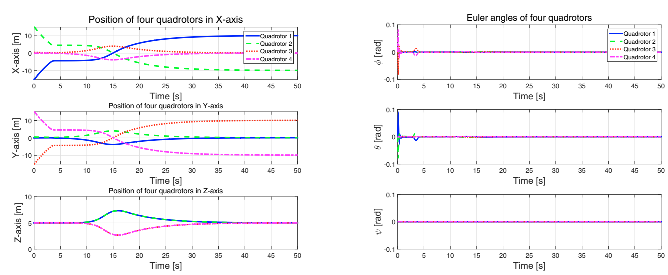

(a) Positions (b) Euler angles

Fig. 5. Positions and Euler angles of four quadrotors

and $\Lambda_{\boldsymbol{\alpha}} = \mathrm{diag}\,[10, 10, 10]$ for each quadrotor-manipulator system. Fig. 3 shows the positions of four quadrotor-manipulator systems at (a) t=0s and (b) t=50s. The final desired formation is formed and the desired angles of manipulators are achieved at the end. Fig. 4(a) shows the trajectories of four quadrotors in X-Y plane. Square represents the initial position of the quadrotor and circle represents the terminal position of the quadrotr. In Fig. 4(a), the quadrotors move in straight lines at the beginning. When they detect each other on the boundary of the detection regions, they change their directions to avoid the collisions and then achieve the final formation. Fig. 4(b) shows the relative distances of four quadrotors. It can be seen that when quadrotors enter the detection region, a repulsive force is appeared to make the quadrotor fly away from the detection region. Therefore, the inter-agent distances are always larger than the smallest safe distance r. Hence, collisions are avoided between quadrotors. Fig. 5(a) shows the positions history of four quadrotors in X,Y,Z-axis. The quadrotors stop and the formation is formed when t is greater than 40s. Fig. 5(b) shows the Euler angles history of four quadrotors. The repulsive forces are generated by corresponding attitudes of quadrotors at the time instants when collisions are being avoided.

5. CONCLUSION

In this paper, we present the kinematics and dynamics of the quadrotor-manipulator system using EL equations. The proposed position controller is able to achieve formation control and collision avoidance. For the attitude stabilization of the quadrotors, we then propose an attitude controller. A distributed manipulator controller is proposed for tracking the desired joint angles cooperatively. The proposed control algorithm is an important step towards developing the next generation of multiple autonomous quadrotor-manipulator systems.

REFERENCES

Arleo, G., Caccavale, F., Muscio, G., and Pierri, F. (2013). Control of quadrotor aerial vehicles equipped with a robotic arm. In *Control & Automation*, 1174–1180.

Chen, G., Yue, Y., and Song, Y. (2013). Finite-time cooperative-tracking control for networked euler-lagrange systems. *Iet Control Theory & Applications*, 7(11), 1487–1497.

Chung, S.J. and Slotine, J.J.E. (2007). Cooperative robot control and concurrent synchronization of lagrangian systems. *IEEE Transactions on Robotics*, 25(3), 686–700.

Graham, A. (1981). Kronecker products and matrix calculus with applications. 1(1), 14.

Khalifa, A., Fanni, M., Ramadan, A., and Abo-Ismail, A. (2013). Adaptive intelligent controller design for a new quadrotor manipulation system. 1666–1671.

Khalil, H.K. (2005). *Nonlinear Systems (Third Edition)*. Prentice Hall.

Lippiello, V. and Ruggiero, F. (2012). Cartesian impedance control of a uav with a robotic arm. In *Robot Control*, 704–709.

Naldi, R., Pounds, P., De Marco, S., and Marconi, L. (2015). Output tracking for quadrotor-based aerial manipulators. In *American Control Conference*, 1855–1860.

Paden, B. and Panja, R. (1988). Globally asymptotically stable 'pd+' controller for robot manipulators. *International Journal of Control*, 47(6), 1697–1712.

Qi, Y., Wang, J., Jia, Q., and Shan, J. (2016). Cooperative assembling using multiple robotic manipulators. In *2016 35th Chinese Control Conference (CCC)*, 7973–7978.

Ren, W. (2009). Distributed leaderless consensus algorithms for networked eulerclagrange systems. *International Journal of Control*, 82(11), 2137–2149.

Siciliano, B., Sciavicco, L., Villani, L., and Oriolo, G. (2009). *Robotics*. Springer London.

Stipanovic, D.M., Spong, M.W., and Siljak, D.D. (2007). Cooperative avoidance control for multiagent systems. *Journal of dynamic systems, measurement, and control*, 129(5), 699–707.

Wang, J. and Xin, M. (2013). Integrated optimal formation control of multiple unmanned aerial vehicles. *IEEE Transactions on Control Systems Technology*, 21(5), 1731–1744.

Yang, H. and Lee, D. (2014). Dynamics and control of quadrotor with robotic manipulator. 5544–5549.